

Synthesis and comparative spectrum properties of nanocrystalline Nd:(Y/Yb)AG

Z. QUNMEI, S. CHANG*

Jinhua Polytechnic, Jinhua, 321007, China

Nanocrystalline Nd:YAG and Nd:YbAG have been synthesized via ammonium bicarbonate co-precipitation methods with doping concentration of 0.5 at.% ~ 4.5 at.%. Different pH and temperature factors were investigated with methods of TG-DSC, XRD, IR, LRS etc. to search optimal formation conditions. A complete transformation was observed at 1100 °C / (pH=8) and 1000 °C / (pH:8-9). The SEM revealed fine dispersion and particle sizes of both. Best performance of nanocrystalline Nd:YAG were achieved when doping with 3 at.% and the novel nanocrystalline Nd:YbAG have no concentration quenching in same range which were learned by results of fluorescence spectrum test.

(Received April 7, 2018; accepted February 12, 2019)

Keywords: X-ray, Fluorescence, Raman spectra, SEM

1. Introduction

Nd:YAG laser as the most commonly used solid-state laser light source, can be achieved a variety of ways such as CW and pulsed operation at room temperature [1]. And transparent ceramics has become the important laser medium material, because its preparation process is relatively simpler than the single crystal growth, and there are many advantages like short preparation period, facilitate the production of large size, easy to control the shape, low economic cost, high doping concentration, good optical homogeneity, multi-functional (for example, laser output and adjusted Q are carried out simultaneously) etc. [2-6]. Therefore, more vigorous driven the synthesis and relevant research work of its raw material i.e. nanocrystalline Nd:YAG. However, nanocrystalline Nd:YAG are still have some drawbacks, such as the phenomenon of concentration quenching, high sintering temperature, low pump light absorption efficiency etc. [7].

With the continuous innovation and development of InGaAs laser diode (LD) pump, Yb³⁺ as the most simple energy level structure active ions, there is no excited state absorption and up conversion, high quantum efficiency [8], low heat load induced by no radiation relaxation, long fluorescence life and other advantages, has become one of modern laser material science research focus [9-11]. And the atomic radius of Yb³⁺ ions is very close to Y³⁺, enabling completely replace Y³⁺ ions within the YAG lattice, then form YbAG self-activating laser material. Thus, a novel self-activated nanocrystalline Nd:YbAG materials prepared by research. Expect it to combine dual advantage of Yb³⁺ and Nd³⁺, weaken the phenomenon of concentration quenching, reduce the sintering temperature, increase the absorption efficiency of the pump light, and enhance the optical conversion efficiency. Thereby enabling the luminescence characteristics of the material to be improved.

Nanocrystalline Nd:(Y/Yb)AG were prepared by ammonium bicarbonate co-precipitation method [12-14], and the influence of pH and calcination temperature on the synthesis of nanocrystalline were mainly studied. These two luminescence characteristics of the basic raw materials for laser transparent ceramics were compared through the test and analysis methods of Thermogravimetric-Differential Scanning Calorimeter (TG-DSC), X-Ray diffraction (XRD), Scanning Electron Microscopy (SEM), Infrared Spectroscopy (IR), laser Raman spectroscopy (LRS), Fluorescence Spectroscopy (FS) etc.

2. Experimental

2.1. Materials

The starting materials were yttria/ytterbium oxide/neodymia (Y₂O₃/Yb₂O₃/Nd₂O₃, 99.999%, Changchun haipurui Rare Earth Material Technology Ltd.), aluminum nitrate nonahydrate (Al(NO₃)₃·9H₂O, AR, Xilong Chemical Co., Ltd.). Ammonium bicarbonate (NH₄HCO₃, AR, Tianjin East China reagent factory) and ammonium sulfate ((NH₄)₂SO₄, AR, Beijing chemical works) were used as the precipitating agent and dispersing agent in the co-precipitation method respectively.

2.2. Synthesis

Accurately calculated the amount of each reagent and weighed according to the stoichiometric ratio of Nd_{3x}:(Y/Yb)_(3-3x)Al₅O₁₂ when Nd³⁺ doping concentration of 0.5 at.%, 1.5 at.%, 2.5 at.%, 3.0 at.%, 3.5 at.%, 4.5 at.%.

The appropriate amount of weighed Nd₂O₃, Y₂O₃ / Yb₂O₃ powders were dissolved in excess 6 mol/L dilute

HNO_3 , mixed together with the $\text{Al}(\text{NO}_3)_3 \cdot 9\text{H}_2\text{O}$ solution which was dissolved in deionized water to form the matrix solution. A precipitating agent solution were prepared through weighed the precipitating agent NH_4HCO_3 in ratio of $n(\text{M}^+):n(\text{NH}_4\text{HCO}_3) = 1:10$ and the dispersing agent $(\text{NH}_4)_2\text{SO}_4$ in 8% of the produce powder mass and thus miscible in an appropriate amount of deionized water.

The reverse strike co-precipitation method used involved homogeneous mixing the matrix solution to the precipitating agent solution in the speed of slower than 2 ml/min which aims to prevent blistering and occurrence of unwanted side reactions. Adjusting the pH of titrated solution to 6,7,8,9,10.

Added the absolute ethanol in volume ratio of 1:8 total solution after titrated, aging for 24 h, suction filtered and rinsed with deionized water and absolute ethanol each three times. The precursor powders were obtained after dried the filtered precipitate at 120 °C for 24 h and grounded it by using agate mortar.

The precursor powders were calcined for 10 h in ceramic crucibles by used a silicon molybdenum rod resistance furnace at temperatures of 800 °C, 900 °C, 1000 °C, 1100 °C, 1200 °C in air atmosphere [15]. Finally, Nd:(Y/Yb)AG nanocrystalline were prepared.

2.3. Performance measurements

Precursor powders were tested for the thermal properties by NETZSCH STA409PC Thermogravimetric-Differential Scanning Calorimeter (TG-DSC), the reference is $\alpha\text{-Al}_2\text{O}_3$, heated from room temperature to 1250 °C, heating rate of 5 K/min. The structure of nanocrystalline were studied by a Japan Rigaku Ultima IV X-ray diffraction analyzer (X-Ray diffraction, XRD), using $\text{CuK}\alpha$ radiation with scanning range $(2\theta) 10^\circ \sim 80^\circ$, $\lambda = 0.15405 \text{ nm}$, X-ray tube voltage of 40 kV, tube current of 20 mA, a scan rate $4^\circ/\text{min}$. Morphology of the samples was observed by utilizing JEOL JSM-6701F field emission scanning electron microscope (Scanning Electron Microscopy, SEM). Frontier FT-IR spectrometer (FT-IR, PerkinElmer, USA) was employed to identify chemical groups and the material structure in the precursors and nanocrystalline. Molecular structural features of the samples is analyzed via Jobin-Yvon HR800 (514.5 nm argon laser light) microscopic laser Raman spectroscopy (laser Raman spectroscopy, LRS). The fluorescence properties of nanocrystalline were investigated through JY Fluorolog-3-tau fluorescence spectrometer (Fluorescence Spectroscopy, 808nm / 980 nm pump source).

3. Results and discussion

3.1. TG-DSC

The mechanism of thermal decomposition and the crystallization temperature of dried Nd:(Y/Yb)AG precursor as studied by TG - DSC are shown in the

thermal analysis curve depicted in Fig. 1. The curves show 40.99 wt% and 62.86 wt% total weight loss for the dried Nd:YAG and Nd:YbAG precursor powders respectively.

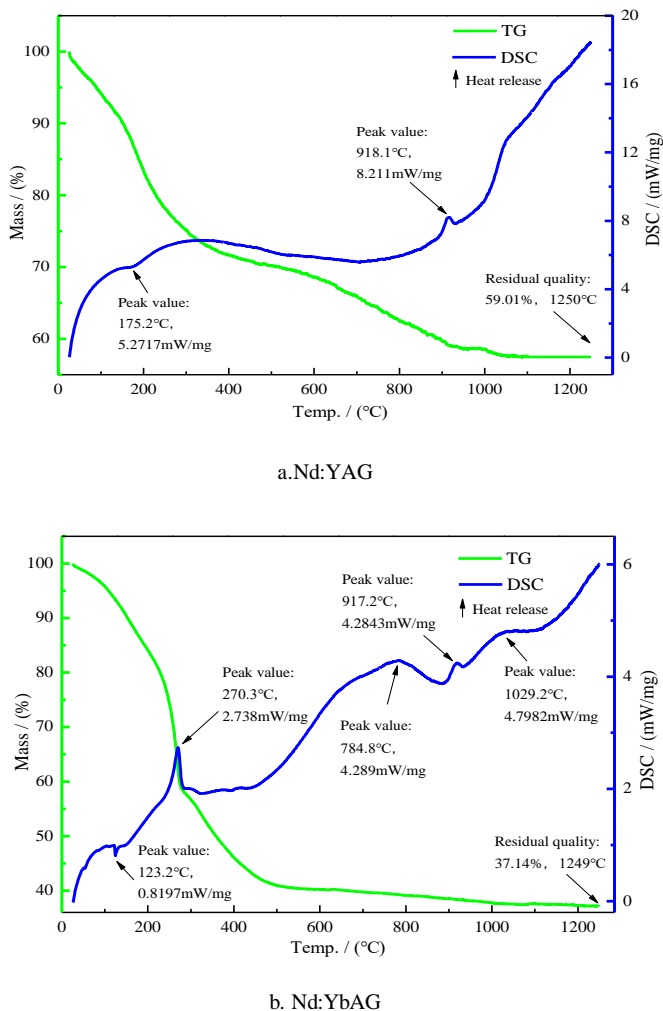


Fig. 1. TG-DSC curve of the Nd:(Y/Yb)AG precursor

In Fig. 1a, Nd:YAG sample with starting weight of 2.864 mg was loaded in TG - DSC crucible. The thermogravimetry curve shows that the mass decreased rapidly below 600 °C due to removal of absorption water (Peak value: 175.2 °C, 5.2717 mW/mg) /nitrate radical/ hydroxyl and decomposition of ammonium and partial carbonate. The thermal decomposition behavior associated with a very large exothermic peak for the Nd:YAG sample as seen in the corresponding DSC curve. The slight endothermic phenomenon from 600 – 850 °C are due to the decomposition of carbonate in the powder which reflect on the TG curve of 7.20% mass loss. The exothermic peak at 918 °C corresponds to the onset crystallization of YAG phase. TG curve leveled off after 1100 °C, this shows that the precursor thermal decomposition process is over, the nanocrystalline Nd:YAG lattice structure become stable.

Fig. 1b shows the TG-DSC curves of Nd:YbAG sample with starting weight of 9.962 mg. Different from

the nanocrystalline Nd: YAG is that the mainly reaction are concentrated before 500 °C, the weight loss up to 59.04 wt% which were mainly caused by the volatilization of physically adsorbed water and crystal water (124.3 °C), the decomposition of NH_4^+ and carbonate (270.3 °C) and the release of remaining NO_3^- , OH^- . The weight loss corresponding to exothermic peak between 750 - 1050 °C are extremely weak, which were represented the process of preliminary forming of YbAG crystal nucleus (784.8 °C), crystallization completely (917.2 °C) and grain growth (1029.2 °C). As the temperature exceeded 1000 °C, the weight loss became imperceptible and the crystalline

phase transition ended, the substances that not entered in crystal lattice have been consumed off during the reaction.

3.2. XRD and SEM

Fig. 2 a and b show the phase evolution as a function of calcination temperature and pH for the nanocrystalline Nd:YAG and Nd:YbAG respectively. The obtained peaks are compared with the corresponding standard JCPDS card No.82-0575 and No.73-1369.

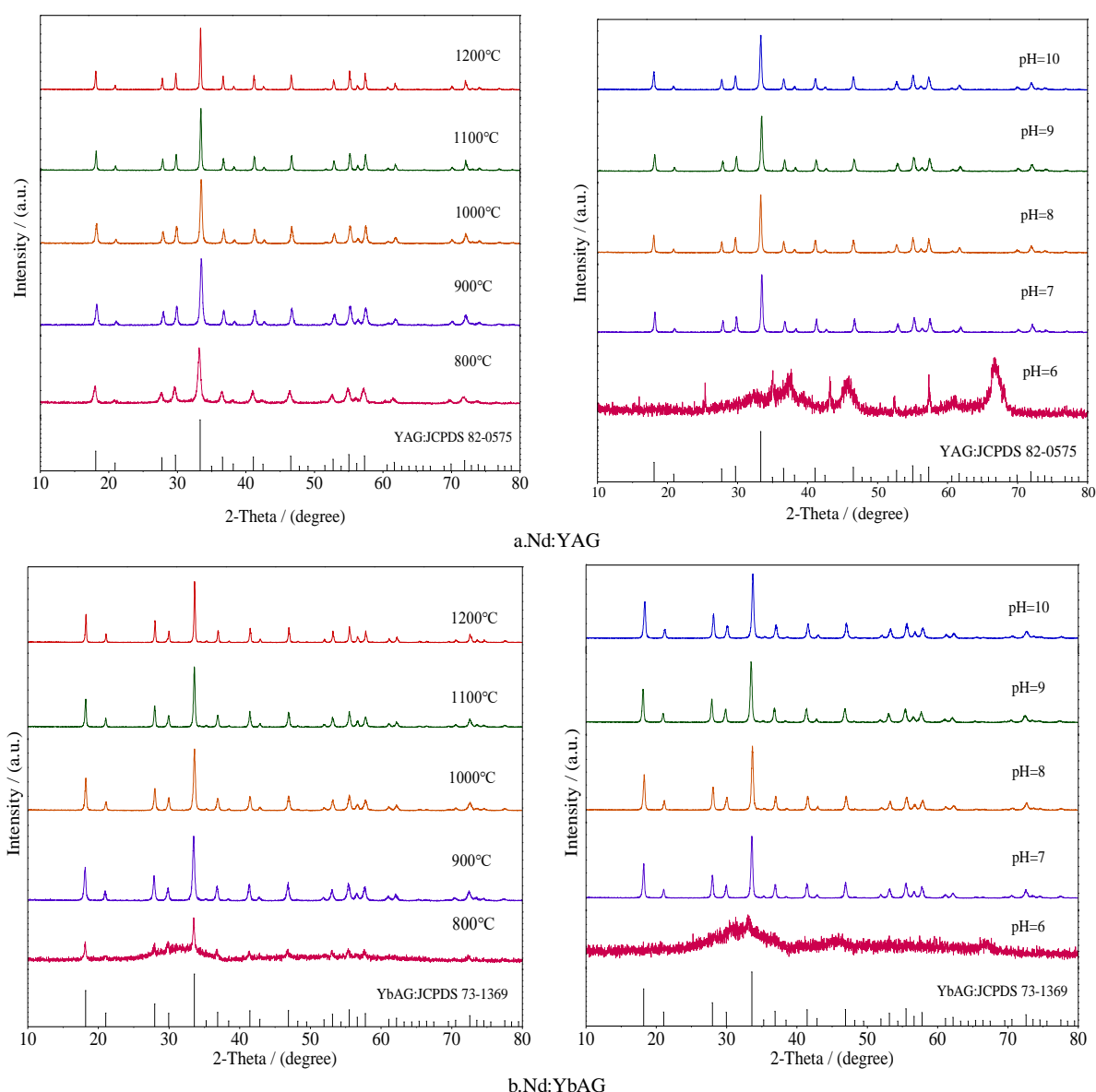


Fig. 2. XRD patterns of nanocrystalline Nd:(Y/Yb)AG phases at different calcination temperatures and pH

XRD patterns of nanocrystalline Nd:YAG when pH set at 8 and calcined at different temperatures as shown in Fig. 2a. The YAG crystal phase has emerged at 800 °C, a more complete crystallization was manifested at elevated temperatures after 900 °C with the phenomenon of peak

shape sharper and narrower FWHM [16]. Distinguished from nanocrystalline Nd:YAG, the phenomenon of nanocrystalline Nd:YbAG is when calcined at 800 °C there are still amorphous state, as shown in Fig. 2b.

Nanocrystalline Nd:YAG and Nd:YbAG which were

prepared in different pH at the same calcination temperature of 1100 °C and 1000 °C, respectively. Its XRD patterns displayed exactly alike that was still in the amorphous state at pH of 6 and the crystalline phase could be formed at a pH above 7.

The scanning electron microscope studies confirm the process of preliminary forming of Nd:(Y/Yb)AG crystal nucleus, crystallization completely, grain growth and densification when calcined at different temperatures.

As it is seen from the images in Fig. 3.a, the best nanocrystalline were observed for the pure Nd:YAG

sample which calcined at 1100 °C with the average partical sizes of 80 nm, meanwhile, the nanocrystalline have been crystallized completely and good dispersion, that's the most suitable state for sintering transparent ceramics [17]. Particles are seen as fine, incomplete crystallization when calcined at 800 °C-1000 °C. The big ingot and crystal layer appeared with the grain recrystallization growth along the nucleus of some large grains at the temperature of 1200 °C, closed pores would emerge if use of the nanocrystalline calcined at this temperature to sinter transparent ceramics.

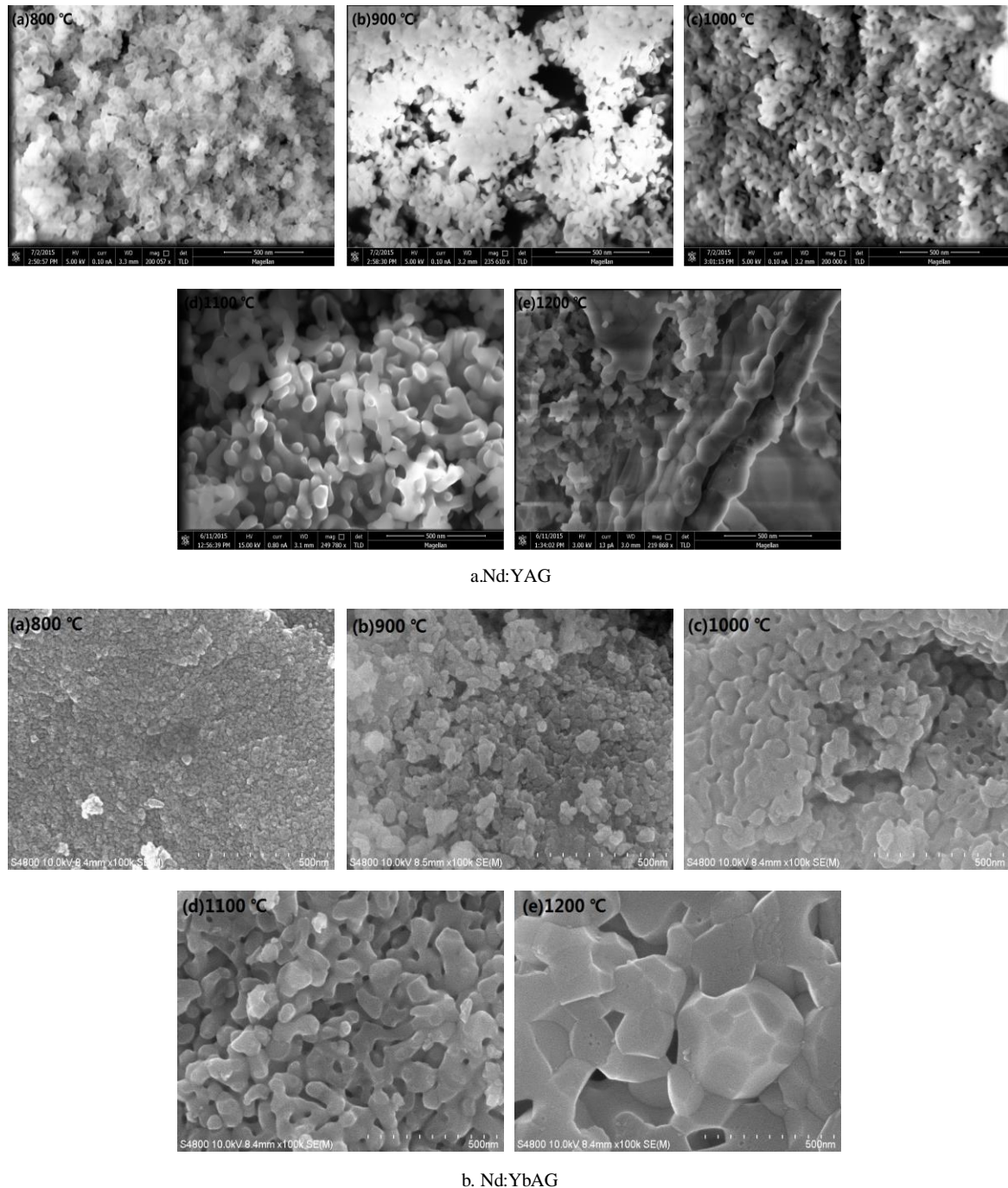


Fig. 3. SEM photos of nanocrystalline Nd:(Y/Yb)AG sintered at different temperatures (800 °C, 900 °C, 1000 °C, 1100 °C, 1200 °C)

Scanning electron micrograph of the nanocrystalline Nd:YbAG derived after calcined at 800°C-1200 °C is seen in Fig. 3b. The particle size is uniform, well dispersion and crystallization completely with the average sizes of 60 nm when calcined at 1000 °C, the good sintering activity were presented. The nanocrystalline were obtained after 800 °C-900 °C calcination, although the particle sizes were small but unevenness, the crystalline phase were formed initially, the crystal grains were not fully developed, the powder particles were not grew enough too. There were particles grew together to form nuclei at 1100 °C, so it is prone to early densified and formed grain boundaries in the process of sintering transparent laser ceramics in the subsequent process and the birefringence or intergranular phase are easy exists between the crystal grains, that will produce the interface reflection and refraction of light,

reducing the optical transmittance and being difficult to achieve the property of transparent. After 1200 °C calcination, the closed pores could appear among the process of crystal grains growth which is not conducive to the ceramic sintering.

3.3. IR

Fig. 4 is an infrared absorption spectra comparison chart between nanocrystalline Nd:(Y/Yb)AG and its precursors prepared by co-precipitation method at different temperatures. The following analysis are obtained after a review of inorganic infrared vibrational frequencies manual and read the relevant literature.

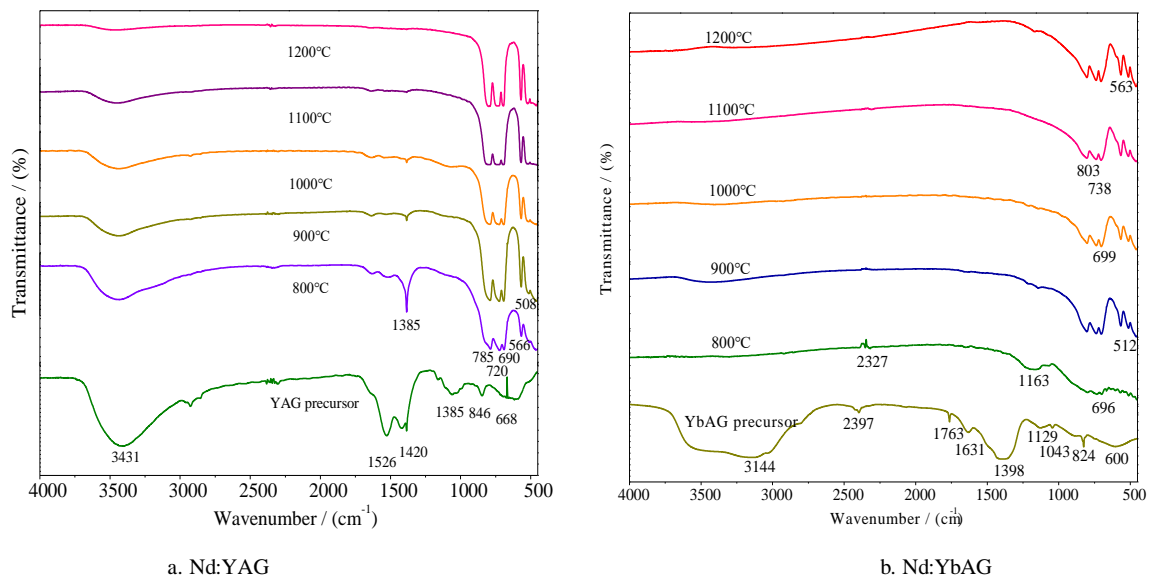


Fig. 4. IR absorption spectra of the Nd:(Y/Yb)AG precursors and nanocrystalline sintered at different temperatures

For YAG precursors, the infrared absorption curve is shown in Fig.4.a, H-O-H bending vibration is happened at the peak in 3431 cm^{-1} , while the absorption peak at 846 cm^{-1} , 1420 cm^{-1} , 1526 cm^{-1} is corresponding to the asymmetric expansion and bending vibration of CO_3^{2-} , the peak at 1385 cm^{-1} shows the asymmetric vibration of NO_3^- , the peak of 668 cm^{-1} is appeared due to the asymmetric absorption of SO_4^{2-} . A series of peaks in the vicinity of 508 cm^{-1} , 566 cm^{-1} , 690 cm^{-1} , 720 cm^{-1} , 785 cm^{-1} are caused by the lattice vibrations and photons interaction of YAG. The infrared absorption spectra in Fig. 4a of nanocrystalline calcined at the temperature 1000 °C and before represents that is still remains the peak at 1385 cm^{-1} corresponding to the asymmetric vibration absorption of NO_3^- , indicating that there are exists NO_3^- even though the YAG crystal phase were already formed and the purity requirements of sintering the Nd:YAG laser transparent ceramics can not be achieved at this time. Combine the analysis in sections 3.1 and 3.2, it was found that the most

suitable calcination temperature for a calcination of Nd:YAG nanocrystalline is 1100 °C.

The spectra of YbAG precursors in Fig. 4b has more absorption peaks compared with YAG. The absorption peaks wherein 3144 cm^{-1} , 1631 cm^{-1} are corresponding to the stretching and bending vibrations of H-O-H, demonstrating that the precursor powder surface containing a small amount of water. The absorption peak at 1763 cm^{-1} reflects the asymmetric vibration of NO_3^- . Vibration of HCO_3^- caused the absorption peak near 2397 cm^{-1} . The presence of CO_3^{2-} ions in precursor and its asymmetric stretching and bending vibration makes the absorption bands produced nearby 1398 cm^{-1} , 824 cm^{-1} . The SO_4^{2-} vibration absorption driven the peak appeared in the vicinity of 1129 cm^{-1} . The absorption band close by 600 cm^{-1} is induced by Al-O bond vibration. The vibration absorption of HCO_3^- near 2327 cm^{-1} and SO_4^{2-} asymmetric absorption peak at 1163 cm^{-1} are still surviving after calcined the YbAG precursors at 800 °C, and that is

echoes with the analysis of not formed Nd:YbAG nanocrystalline phase at 800 °C in 3.2 section. A series of peaks at 512 cm^{-1} , 563 cm^{-1} , 699 cm^{-1} , 738 cm^{-1} , 803 cm^{-1} are caused by YbAG lattice vibrations and photons interactions. Infrared spectra of Nd:YbAG nanocrystalline were calcined between 900 °C-1100 °C explained that NO_3^- , HCO_3^- , CO_3^{2-} , SO_4^{2-} or other ions have been decomposition after calcined, the crystal water and adsorbed water have been evaporated together. Consideration of economic factors and comprehensive analysis with the sections of 3.1 and 3.2, thus determined that 1000 °C is most appropriate calcination temperature of Nd:YbAG nanocrystalline.

3.4. LRS

Fig. 5 is Raman spectra of nanocrystalline Nd:(Y/Yb)AG. Wherein Fig. 5.a is the Raman spectra of nanocrystalline Nd:YAG (known by the analysis of section 3.3) at its optimum calcination temperature 1100 °C. Vibration attribution of Raman peaks were conducted by reference on literature [18-23], the Raman peaks at 162 cm^{-1} , 218 cm^{-1} , 260 cm^{-1} , 338 cm^{-1} , 370 cm^{-1} , 402 cm^{-1} , 716 cm^{-1} , 782 cm^{-1} , 980 cm^{-1} , 1046 cm^{-1} , 1122 cm^{-1} are induced by the vibration of YAG lattice, which were mainly corresponds to the mixing function of translational vibration and rotational vibration of Y^{3+} and asymmetric stretching vibration of (AlO_4) tetrahedral, the main peak position is at 1122 cm^{-1} .

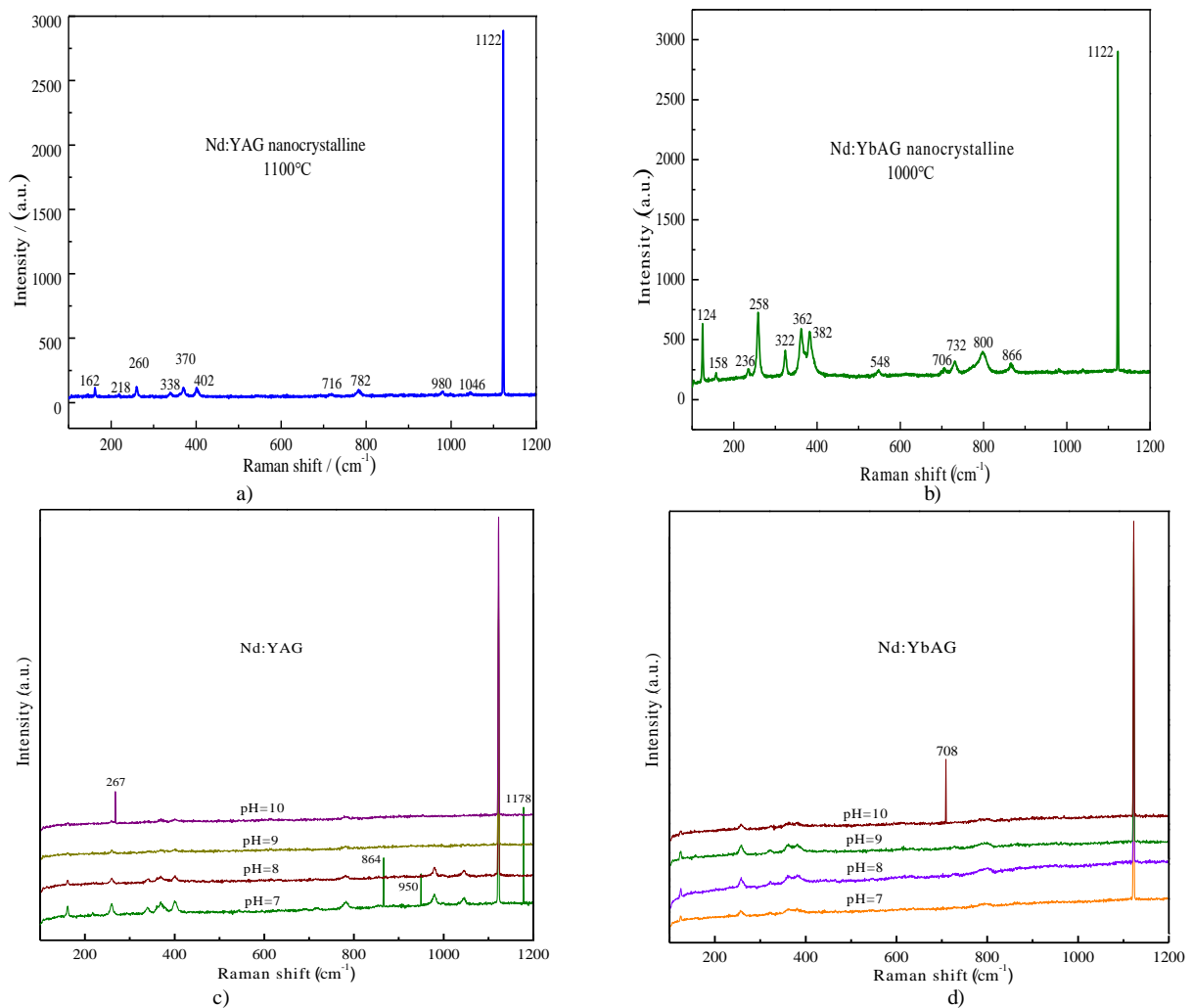


Fig. 5. Laser Raman spectra of nanocrystalline Nd:(Y/Yb)AG

Raman spectra of Nd:YbAG nanocrystalline calcined at the most appropriate temperature 1000 °C (known through analysis of section 3.3) are shown in Fig. 5b, due to the vibration of YbAG lattice, a series of peaks of 124 cm^{-1} , 158 cm^{-1} , 236 cm^{-1} , 258 cm^{-1} , 322 cm^{-1} , 362 cm^{-1} , 548 cm^{-1} , 706 cm^{-1} , 732 cm^{-1} , 800 cm^{-1} , 866 cm^{-1} , 1122 cm^{-1} were observed, the main peak position is similar with Nd:YAG nanocrystalline of 1122 cm^{-1} . The peak nearby

124 cm^{-1} , 158 cm^{-1} , 236 cm^{-1} , 258 cm^{-1} , 322 cm^{-1} , 362 cm^{-1} , 548 cm^{-1} , 706 cm^{-1} , 732 cm^{-1} , 866 cm^{-1} , 1122 cm^{-1} are parallelism of Yb^{3+} lattice translational vibration, rotational vibration and asymmetric stretching vibration of (AlO_4) tetrahedral; the peak at 800 cm^{-1} is mainly related with symmetry stretching vibration and asymmetric bending vibration of (AlO_4) tetrahedral.

Laser Raman spectra of nanocrystalline Nd:YAG

prepared at 1100 °C with the pH of 7-10 is displayed on Fig. 5c. There are sharp Raman peaks appeared at 864 cm^{-1} , 950 cm^{-1} , 1178 cm^{-1} when pH value is at 7 which are corresponding to the bending vibration of carbonate ions, asymmetric stretching vibrations of O = N = O bonds, asymmetric stretching vibration of S = O, the atoms of C, N, S are still residual in YAG lattice due to the rare earth nitrate solution was insufficient reacted with ammonium bicarbonate precipitant in a neutral environment. In addition to the main peak at 1122 cm^{-1} , the other base peak are weak at pH of 9, that is represents incomplete crystallization. The peak of 267 cm^{-1} is caused by Al-O bending vibrations at pH of 10, which is due to Al^{3+} are precipitated prior to Y^{3+} while failed to precipitated homogeneous in strong alkaline environment, causing the segregation of Al-O composition in lattice structure and then the sharp Raman miscellaneous peak are arisen. The Raman vibration peaks are conform to the preparation requirements of Nd:YAG nanocrystalline without hetero peaks after belonging to the right peak position, so the most suitable pH value is 8.

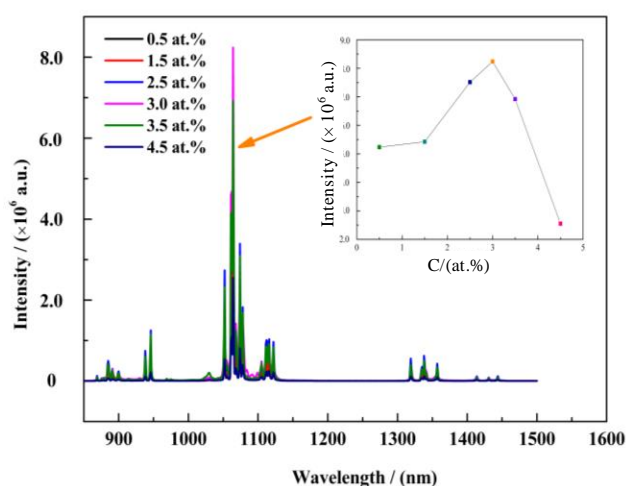
The laser Raman spectra of nanocrystalline Nd:YbAG which were prepared at pH of 7-10 with the calcination temperature of 1000 °C are shown in Fig. 5d. The base

peak of nanocrystalline Nd:YbAG are not obvious at pH value 7, although the YbAG crystal phase were already formed but incomplete under neutral conditions, the vibration intensity of molecular bond is not high enough with poor sintering activity. The peak at 708 cm^{-1} wherein Fig. 5d at pH value 10 was generated by O = N = O and ON = O bending vibration, and the nanocrystalline Nd:YbAG prepared at this time can not meet the purity requirements. There are purity laser Raman spectrum peaks of nanocrystalline Nd:YbAG when synthesize at pH 8-9, the preparation conditions within this pH range are suitable for the requirements.

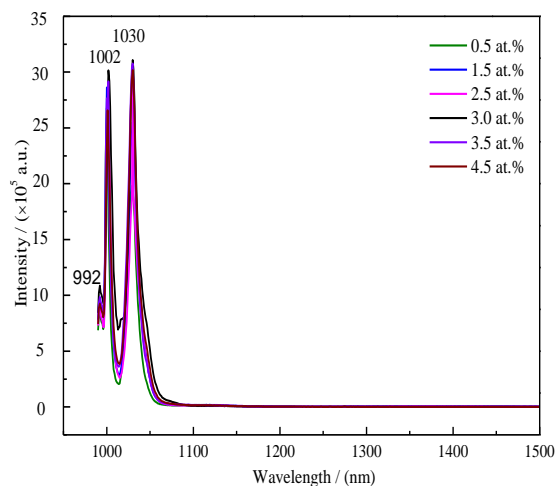
The results of laser Raman spectrum test under different pH in the range of 7-10 has been supplemented with the XRD analysis in section 3.2, indicates the optimum pH conditions of nanocrystalline Nd:YAG and Nd:YbAG are 8 and (8-9) respectively.

3.5. Fluorescent spectroscopy

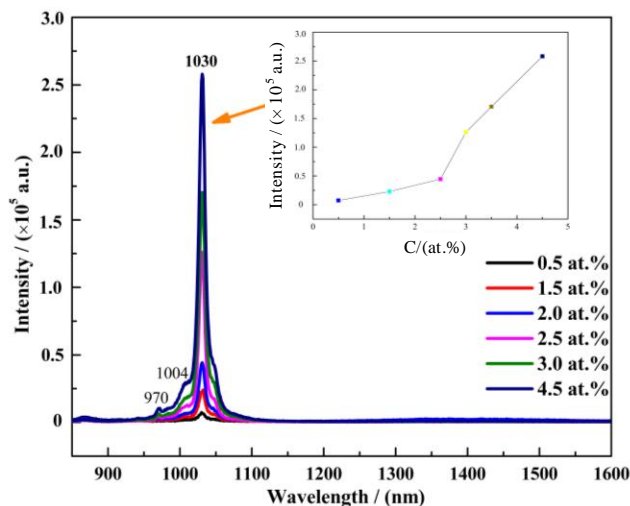
The fluorescence spectra of nanocrystalline Nd:(Y/Yb)AG at different doping concentration at 0.5 at%, 1.5 at%, 2.5 at%, 3.0 at%, 3.5 at%, 4.5 at% were exhibited in Fig. 6.



a. Nd:YAG(808 nm)



b. Nd:YbAG(980 nm)



c. Nd:YbAG(808 nm pump)

Fig. 6. Fluorescence Spectra of nanocrystalline Nd:(Y/Yb)AG

Fig. 6a is fluorescence spectra of nanocrystalline Nd:YAG which were pumped by 808 nm laser source, the highest peak arisen at 1064 nm with the control of Nd^{3+} energy transition at ${}^4\text{F}_{3/2}\text{-}{}^4\text{I}_{11/2}$, but with Nd^{3+} doping concentration increases, the fluorescence intensity is not gradually increased, but there has been a concentration quenching phenomenon [24], while the best fluorescence intensity were obtained when doping with neodymium of 3 at% [25, 26].

Look into the Fig. 6b that fluorescence spectra of Nd:YbAG nanocrystalline using 980 nm pump excitation, theoretically the emission peak of Yb^{3+} , Nd^{3+} should appear in the vicinity of 1030 nm and 1064 nm, respectively. But there are strong peaks in the vicinity of 1002 nm and 1030 nm observed in the measured spectra, actually the theoretically peak at 1064 nm of neodymium ions was not appeared. There is no difference when judging from the number of emission peaks with the theoretical peaks, but a blue shift phenomenon that the whole spectrum shifted to the shorter wavelength about 30 nm has been happened. Analyze the reasons may be due to the energy band renormalization effect caused by defects such as electron-hole, and that can transform the energy gap between ground state and excited state and thus driven the absorbed or emitted photons energy to change, then the migration of fluorescent emission point resulting in blue shift for fluorescence spectra of nanocrystalline Nd:YbAG samples.

A weak and a strong peak appeared nearby 992 nm, 1002 nm were shown in Fig. 6b which corresponds to the energy level transition of Yb^{3+} between ${}^2\text{F}_{5/2}\text{-}{}^2\text{F}_{7/2}$. Strong peak at 1030 nm was caused by energy level transition of Nd^{3+} between ${}^4\text{F}_{3/2}\text{-}{}^4\text{I}_{11/2}$ [27]. Compared to Fig. 6a of the fluorescence spectra for nanocrystalline Nd:YAG, because of the active Yb^{3+} ions absorbed and stored partial energy, thus the fluorescence intensity decreased to some extent.

The fluorescence spectra of nanocrystalline Nd:YbAG excited by 808 nm pump are represent in Fig. 6c, the graphic display the emission peaks are located at 970 nm (weak), 1004 nm (weak), 1030 nm (strong). Contrast to Fig. 6a, in addition to the main peak at 1064 nm, there are still have many other weak emission peaks of Nd:YAG nanocrystalline, and that will play a negative impact on the luminous efficiency of the material. But for nanocrystalline Nd:YbAG, the emission peaks are more simpler, by the way, only centered around 1030 nm, so the energy conversion is more efficiently, which makes a contribution to improve the materials luminescence efficiency. Combined with the analysis for Fig. 6b, the peak at 1030 nm is surely corresponds to fluorescence excitation of Nd^{3+} [28]. The function between concentration of doping neodymium ions and the the strongest emission peak was depicted in the illustrations of Fig. 6c, along with the increase of Nd^{3+} doping concentration, the excitation intensity of Nd^{3+} enhanced under the effective co-ordination between Yb^{3+} and Nd^{3+} , the fluorescence intensity didn't reduced, therefore, in the range of neodymium ion concentrations for 0.5 at% - 4.5 at%, the novel material namely nanocrystalline Nd:YbAG

successfully avoid the phenomenon of concentration quenching.

4. Conclusions

Nanocrystalline Nd:YAG and Nd:YbAG with neodymium ion doping concentration different from 0.5 at.% ~ 4.5 at.% were prepared by co-precipitation method used ammonium bicarbonate as precipitant agent. Tested analysis of TG-DSC, XRD, SEM, IR, LRS, FS indicated that the structure of each sample are in line with yttrium aluminum garnet and ytterbium aluminum garnet, the optimum calcination temperature with the order of nanocrystalline Nd:YAG and nanocrystalline Nd:YbAG is 1100 °C and 1000 °C and the most appropriate pH value is 8,8-9, respectively. In terms of the nanocrystalline Nd:YAG, a traditional materials, the best fluorescence performance near infrared was observed when Nd^{3+} doping concentration of 3.0 at.%, which is corresponding to the energy level transition between ${}^4\text{F}_{3/2}\text{-}{}^4\text{I}_{11/2}$ of Nd^{3+} , while there do exists a phenomenon of concentration quenching. However, the novel materials for nanocrystalline Nd:YbAG have a serious of advantages like better control of the preparation process, lower calcination temperature, no concentration quenching in the same neodymium doped range of 0.5 at.% -4.5 at.%, simpler energy level structure, higher luminous efficiency. This is indeed a kind of the novel excellent available raw materials for laser transparent ceramic.

Acknowledgements

The work was partially supported by Changchun Science and Technology Project with the number of 14KP017 and 14GH011. The authors would like to thank Optoelectronic Functional Materials Engineering Research Center of the Ministry of Education in Changchun University of Science and Technology for their financial and moral support to carry out this work. We thank Mr. Zhao of Physics and Chemistry Scientific Experiment in University of Science and Technology of China for providing FS data for our samples. The authors are grateful to Mr. Li with Jilin University for help in laser Raman spectra test. The authors also thank colleagues in the Changchun University of Science and Technology for their kind help in TG-DSC, XRD, SEM, IR measurements and support during this project.

References

- [1] J. Sanghera, B. Shaw, W. Kim et al., SPIE Lase, International Society for Optics and Photonics 1781 (2011).
- [2] B. Liu, J. Li, R. Yavetskiy et al., Journal of the European Ceramic Society **35**(8), 2379 (2015).

- [3] Yihua Huang, Jiang Dongliang, Zhang Jingxian et al., *Journal of Rare Earths* **31**(2),153 (2013).
- [4] L. Wen, X. Sun, Z. Xiu et al., *Journal of the European Ceramic Society* **24**(9), 2681 (2004) .
- [5] Liu Wenbin, Preparation, "Microstructure and laser properties of Nd:YAG transparent ceramics,," Shanghai Jiao Tong University, 2012.
- [6] V. Lupei, *Optical Materials* **31**(5), 701 (2009).
- [7] A. Verma, N. Malhan, A. K. Ganguli, *Materials Letters* **81**, 242 (2012).
- [8] D. Fagundes-Peters, N. Martynyuk, K. Lunstedt et al., *Journal of Luminescence* **125**(125), 238 (2007).
- [9] X. J. Zhang, C. Li, D. X. Huang et al., *Applied Mechanics & Materials* **697**, 31 (2015).
- [10] Y. Cheng, J. Lv, S. Akhmalaliev et al., *Optical Materials Express* **4**, 100 (2015).
- [11] G. Nemova, R. Kashyap, *Journal of Luminescence* **99** (2015).
- [12] W. Zhang, T. C. Lu, N. Wei et al., *Materials Research Bulletin* **365** (2015).
- [13] P. Ramanujam, B. Vaidhyanathan, J. Binner et al., *Ceramics International* **40**(3), 4179 (2014).
- [14] G. Xu, X. Zhang, W. He et al., *Materials Letters* **60**(7), 962 (2006).
- [15] R. Malekfar, S. Arabgari, *Current Applied Physics* **11**(4), 1077 (2011).
- [16] E. Caponetti, S. Enzo, B. Lasio et al., *Optical Materials* **29**(10), 1240 (2007).
- [17] R. Yang, J. Qin, M. Li et al., *Journal of the European Ceramic Society* **28**(15), 2903 (2008).
- [18] S. Kostić, Z. Ž. Lazarević, V. Radojević et al., *Materials Research Bulletin* **63**, 80 (2015).
- [19] Yu Jinqiu, Cui Lei, He Huaqiang et al., *Journal of Rare Earths* **32**(1), 1 (2014).
- [20] Su Jing, Q. L. Zhang, S. T. Yin et al., *Spectroscopy and Spectral Analysis* **29**(6), 1577 (2009).
- [21] Dong Kun, "Preparation and molecular Raman spectral analysis of Nano silver enhancement substrate," Kunming University of Science and Technology, 2011.
- [22] L. J. Liu, H. Zhou, Q. Dong-Sheng et al., *Atomic Energy Science & Technology* **43**(2), 103 (2009).
- [23] W. Zhu, L. Huang, J. Chen et al., *Journal of Synthetic Crystals* **41**(4), 834 (2012).
- [24] M. O. Ramirez, J. Wisdom, H. Li et al., *Optics Express* **16**(9), 5965 (2008).
- [25] Y. Zhydachevskii, I. I. Syvorotka, L. Vasylechko et al., *Optical Materials* **34**(12), 1984 (2012).
- [26] C. Jacinto, A. Benayas, T. Catunda et al., *Journal of Chemical Physics* **129**(10), 70 (2008).
- [27] Z. Wang, B. Zhang, J. Ning et al., *Chinese Optics Letters* **13**(2), 021403 (2015).
- [28] J. Zang, Y. Zou, Y. Song, *Journal of the Chinese Ceramic Society* **37**(8), 1338 (2009).

*Corresponding author: nacc0509@aliyun.com